Sodium aluminate-catalyzed synthesis of biodiesel

Giovanni Pampararo[1], *Damien P. Debecker*[1]*

1. Université catholique de Louvain (UCLouvain), Institute of Condensed Matter and Nanosciences (IMCN), Place Louis Pasteur 1, Louvain-la-Neuve, 1348, Belgium
* damien.debecker@uclouvain.be

KEYWORDS: $NaAlO_2$, Biodiesel, Transesterification, Renewable energy, Heterogeneous catalyst

ABSTRACT: Fatty acid methyl esters (FAME) were produced with high efficiency by a cheap, available, and strongly basic catalyst: $NaAlO_2$ (SA). A deep characterization revealed that both basic density and strength played a crucial role in the transesterification reaction. Its catalytic performances were compared with other classical basic catalysts, in the same operative conditions and the outline is that SA outcompetes all other benchmarks in terms of specific activity and final FAME yield. SA is also truly heterogeneous (does not leach).

INTRODUCTION:

Fossil fuel dependence is nowadays at the heart of many international debates, ranging from environmental to geopolitical issues. Additionally, in developing nations, economies are expanding and are charcaterized by an enormous energy demand. To reduce environmental footprints, gas emissions and chemical derived pollution it is clear that renewable energy and biofuels play a pivotal role in modern society [1]. In this field, catalysts science is essential to drive the transition from fossil fuel based technologies to biofuels based ones, in particular those derived from biomass feedstock as 2nd and 3rd generation sources i.e. non-edible oils, waste cooking oils, and algal biomass. Among the biofuels, biodiesel is a formidable candidate to promote sustainability and circular economy. It is biodegradable, less toxic, and it needs less purification and separation steps because it doesn't contain nitrogen or sulfur[2]. Namely, it is a mixture of fatty acid methyl esters (FAME)[3] and it is principally synthesized, at an industrial level, through the transesterification of triglycerides via a homogeneously catalyzed process. However, this route has a strongly limited feedstock flexibility due to unwanted

side reactions, such as soap formation if free fatty acids (FFA) and water content are > 0.5% and > 0.06 wt%, respectively[4]. Common catalysts as KOH, NaOH are largely available and cheap, however, the application is severely restricted by high recycle cost, soap formation and consequent loss of yield and problems of products separation[4,5]. Acid homogeneous catalysts as HCl and H_2SO_4 can be also employed because they are not affected by the FFA content present in the feedstock, and they can simultaneously catalyze esterification and transesterification reactions[6]. However, the concomitant esterification, between the alcohol and the FFA, produces water and can inhibit the reaction, other drawbacks are the corrosions and hazardous problems as well the increment cost due to a necessary higher alcohol to oil molar ratio.

Heterogeneous catalysts are more attractive because they have more tolerance to the feedstock purity, they are more environmentally friendly because they can be recovered, regenerated, and reused reducing also plant costs[5]. Tremendous efforts have been carried out by researchers to obtain efficient catalyst. Among the heterogeneous base catalysts KF/ZnO[7] , K/KOH/Al_2O_3[8], K/TiO_2 [9], MgO based catalysts[10–12], CaO based catalysts[13–16] and hydrotalcite like materials[17–20], have been extensively studied. Although solid catalysts have clear favorable characteristics, their preparation is often associated to non-cost effective synthesis procedures, time consuming steps as pretreatments or preparation/storage activities. Highest is the production cost, highest will be the investment cost and the time to recover it. Moreover, according to green chemistry, highest is the number of steps the lowest will be the possibility to have an environmentally sustainable process. Nevertheless, mainly because of raw material and precursor costs, deactivation and/or leaching, an industrial perspective is still far from being effective. This led us to investigate a new promising candidate among heterogeneous base catalysts.

Sodium Aluminate (SA), $NaAlO_2$, is an inexpensive inorganic compound that is mainly in demand for water purification[21]. Nowadays, its use is also found in paper industry, paint pigment, detergents[22]. It can be easily prepared by reaction between sodium hydroxide and aluminum hydroxide. However, what really matters is that SA is contained in several wastes of alumina-based industry (catalysts synthesis, thermally stable materials production etc.), it is a byproduct of industrial boehmite synthesis, and it is present in Bayer process wastewaters[23]. It follows those low-cost resources to be recycled for the sodium aluminate synthesis are largely available. In fact, SA is a suitable candidate to be employed in the catalysis field, in particular for the transesterification reaction, because it is a solid strongly basic material, it is cheap, immiscible with reaction media, and it can be easily recovered.

Quite recently, it has been successfully employed as catalyst for carboxymethylations[24,25], glycerol carbonate synthesis [26–28] and aminothiophenes[29]. Moreover, Kessler et al.[30,31] synthesized mesoporous alumina-sodium aluminate materials by sol gel technique and Ning et al[32] produced sono-modified halloysite nanotube with $NaAlO_2$ for transesterification reaction. Although these catalysts may be efficient, it is difficult to think and plan an effective industrial scale up to supply the always rising request of fuels. Furthermore, at the best of our knowledge, only sparse works have been found in literature for the commercial material[33–35] applied to biodiesel production and a lack of knowledge has been found in comprehensive understanding of material properties and related catalytic activities.

In the effort to find a feasible and sustainable catalyst for the chemical industry of biodiesel, we deeply characterize and test sodium aluminate for the transesterification reaction. Attempting to cover another lack in the sector, SA is reported and compared, in the same catalytic conditions and with the same activity parameters, with strongly basic catalysts already found in literature. These materials have been chosen as benchmark candidates because they are cheap, available and they can be quite easily reproduced in the synthesis. Finally, they belong to the principal categories of studied base catalysts for the transesterification reaction.

EXPERIMENTAL SECTION

Catalysts preparation

Sodium aluminate (SA): Sodium aluminate (Sigma Aldrich, Na 40-45%, Al 50-56%) powders were calcined in a muffle furnace under static air firstly at 393 K for 3 hours, then at 723 K for 5 hours with a heating ramp of 5 K/min. Calcined catalyst was stored, sealed and closed into a desiccator.

Strontium oxide (SrO): SrO has been synthesized following procedural details reported in ref.[36]. Briefly, powders of $SrCO_3$ (Roth, ≥98%) have been calcined at 1473 K for 5 hours (2 K/min) under a gentle air flow in a tubular furnace. According to the reference no storage precautions have been foreseen, thus, for better comparison and reproducibility, the calcined powders have been stored sealed and closed into a desiccator.

Calcium Oxide (CaO): CaO has been prepared according to ref.[37]. Briefly, $CaCO_3$ (Acros Organics, ≥98%) powders have been calcined at 1273 K for 3 hours, 3 K/min. The so obtained oxide was then heated with distilled water, under reflux conditions, at 333 K for 6 hours. The sample was filtered, washed and dried overnight at 393 K. Subsequently, the dried powders have calcined at 473 K for 3 hours, 5 K/min. Being that in the reference precautions have been considered to avoid possible site

contamination by CO_2 and H_2O, the sample have been sealed and stored at 353 K under vacuum conditions.

Potassium iodide impregnated over alumina (KI_A): KI_A has been synthesized similarly to ref.[38] the best catalyst found has been reproduced. Firstly, commercial boehmite has been dried at 373 K for 9 hours, 2 K/min, then it has been calcined at 823 K for 5 hours, 5 K/min. By wet impregnation technique, the desired amount of KI was introduced with an aqueous solution containing KI (Roth, ≥ 99%), to finally obtain a 35% wt loading respect to the previously obtained γ-Al_2O_3. After drying, the catalyst has been calcined at 773 K for 3 hours, 5 K/min.

Calcined Hydrotalcite (CHT): According to reference[39] the hydrotalcite like catalyst has been synthesized by coprecipitation at high supersaturation, with the same reported procedure,in agreement with the best catalyst obtained in the reference. Briefly, two solutions, A and B, were first prepared and heated to 313 K. Then they were added simultaneously to a beaker under vigorous stirring. Solution A (100 ml) was prepared by mixing saturated solutions of $MgNO_3$ * 6 H_2O (Roth, ≥98%) and $AlNO_3$*$9H_2O$ (Merck, ≥98.5%) with the molar ratio equal to 3. Solution B (100 mL) was prepared by dissolving 0.17 mol of sodium hydroxide (Sigma Aldrich, ≥97%) and 0.075 mol of sodium carbonate (Roth, ≥99.5%) in distilled water. After 2 h, the precipitates were aged at 338 K under reflux conditions. The product was then filtered, washed thoroughly with deionized water and dried at 363 K for 24 h. The powders were calcined at 773 K for 7 hours.

Characterizations techniques

XRD patterns have been recorded using a Bruker D8 Advance diffractometer (Bragg–Brentano geometry). Cu is employed as Kα source (λ=0.15418 nm) at 1200 W (30 mA, 40 kV). Diffraction patterns have been acquired with the parameters as here reported: 2θ range 5°-80°, step size 0.05° (2θ) and 1.5 s each step. The detector was a Bruker Lynxeye XE-T. Identification of the phases was carried out using Pearson Crystal Database (PCD) software.

N_2 -physisorptions have been carried out at 77 K using a Micrometrics Tristar 3000 instrument. Before every analysis, the calcined catalysts were degassed overnight under vacuum at 443 K. The Brunauer-Emmett-Teller (BET) model was used to calculate the Specific Surface Area (SSA, m^2/g) in the relative pressure range of 0.05–0.30. Total pore volume (V_p) was estimated from the adsorption branch of the isotherm at p/p_0=0.98 and the average pore diameter (D_p) was estimated from the BJH model applied on the desorption isotherms.

Infrared (IR) spectra were recorded with a Bruker Equinox 55 spectrometer from 400 cm^{-1} to 4000 cm^{-1}. Backgrounds have been recorder in air. The samples were pressed into thin wafers with KBr

and spectra were recorded using 0.5 wt.% of the sample in KBr, total mass 0.500 g). Spectra have been collected with 140 scans and a resolution of 4 cm^{-1}. DRIFT studies have been pursued on the same instrument: the background has been collected each time with a aluminum mirror, a first drift spectrum has been recorded on the previously dried, at 393 K, catalysts immediately after the placement in the dome. Then, the sample was heated to 673 K in He flow and held at this temperature for 1 h in order to remove weakly adsorbed basic species. After cooling to 333 K, another drift spectrum was recorded. The subtraction spectra have been obtained subtracting the second recorded spectrum to the first one. After that, carbon dioxide was introduced into the cell with a 50% v/v mixture, He balanced, for 30 min. A spectrum has been recorded each minute for 30 min. Then, a He flow was admitted flushing the cell, spectra of adsorbed CO_2 were recorded using the same previously reported conditions.

Carbon dioxide temperature-programmed desorption (TPD) experiments were conducted using a CATLAB instrument, from Hiden equipped with QGA mass spectrometer for gas analysis. 60 mg of each sample were loaded in a quartz reactor supported by quartz wool and degassed at 673 K for 1h using a heating ramp of 10 K/min in flowing helium (50 mL/min). Next, the samples were cooled to 333 K and exposed to a 15% CO_2-Ar (50 mL/min) mixture for 90 min. the samples were finally purged in flowing Ar for 90 min at 333 K. During the proper TPD experiments, the samples were heated up to 1073 K using a heating rate of 5 K/min and a Ar flow of 50 mL/min. The amount of desorbed CO_2 was obtained by integration of the desorption profiles and referenced to the calibrated signals for known volumes of analyzed gases.

Catalytic tests

In each catalytic test, the transesterification reaction was carried out in the batch mode, in a 100 mL double-necked round bottom flask with a stirrer and a reflux condenser in a silicon oil bath. The temperature of the bath was set to 333 K. Because of the hygroscopic nature of the materials, before each test, the catalysts were previously overnight dried at 393 K to remove the moisture.

First, the catalyst, 5% wt respect to the oil mass, is left with the methanol (Alfa Aesar, ≥ 99%), 10/1 methanol/oil molar ratio, to produce excellent reflux conditions, homogeneous temperatures and to react and produce the methoxide species for 45 min. In parallel, 5 g of sunflower oil, bought in a local supermarket, were heated at 353 K to remove the moisture. Secondly the hot sunflower oil has been added to the basic mixture and allowed to react for the desired time i.e. 20 min, 60 min, 120 min, 180 min, 240 min. Finally, the catalyst was separated from the liquid by centrifugation at 10000 rpm for 10 min. For the injection mix., 100 mg of the reacted mixture was diluted in n-Hexane (Roth, ≥ 99%)

and 500 μL of the internal standard (Octyl acetate (Sigma Aldrich, ≥ 99%), 17 mg/mL) have been added.

The samples so obtained were analyzed with a Gas Chromatograph (GC-FID) Bruker SCION 456 equipped with a Agilent IU DB-FATWAX 30 m, 0,25 mm, 0,25 um column. Injector temperature was set at 523 K with a split ratio of 20. Oven temperature was raised with a 10 K/min ramp from 423 K to 513 K. FID temperature was set at 523 K. All the Fatty acid methyl esters (FAME) involved in the reaction have been calibrated by using a FAME MIX (certified reference, F.A.M.E. Mix, C4-C24, Supelco) and calculating response factors. According to the sunflower oil composition (palmitic acid, stearic acid, ooleic acid, linoleic acid), the main detected peaks were: methyl palmitate (C17:0), Methyl palmitoleate (C17:1), Methyl stearate (C19:0), Methyl oleate/Methyl elaidate (C19:1n9 trans + cis) and Methyl linoleate/Methyl linolelaidate (C19:2n3 + C19:2n6). The biodiesel yield has been evaluated as follow:

FAME Yield (FY%): Σ: C_{out} FAME (mg/mL) / C_{mix} (mg/mL)

Where C_{out} is the sum of the evaluated quantities by calibration, C_{mix} is the concentration of the reaction mix in the injection solution and it corresponds to 20 mg/mL. Every injection was repeated 3 times and values were averaged.

Leaching tests have been carried out rapidly removing, by mean of the centrifugation, the catalyst after 20 min of reaction. The mixture (without any solids) was then left to react for 60 min, 120 min, 180 min, 240 min. Each time, 100 mg of the mixture were collected with a syringe and treated to be analyzed via GC-FID. If the FY% is not increased after the catalyst's removal, reaction is stopped, and no homogeneous species are present in the reaction mixture.

Free Fatty Acids (FFA) content has been evaluated by titration. 500 mg of the reaction mix have been diluted in 10 mL of 2-propanol (VWR, ≥ 99.8 %), then Phenopthalein (Roth, ≥ 99%) has been chosen as indicator of the titration and a 0.5 % (m/v) solution has been prepared. 4 drops of the indicator solution have been added and a NaOH solution 0.025 M has been added drop by drop until the solution toning. Each measure was replicated at least 3 times and averaged.

Reusability test have been carried out as follow: The catalytic reaction was pursued for 60 min, with the previously mentioned operative conditions, then after centrifugation, the catalysts was furtherly separated and washed with Methanol and n-hexane by filtration. The powders were dried for 60 min at 393 K and calcined at 723 K for 60 min. After cooling the recovered catalyst was tested in the same conditions for 3 additional times.

RESULTS AND DISCUSSION

Catalysts characterization

In Figure 1 the X-Ray diffraction (XRD) patterns of the studied catalysts are reported. Looking at SA pattern the calcination successfully removed the hydrated phase, namely $NaAlO_2$*4/5 H_2O, furthermore, no presence of dawsonite phase was detected. Then, SA presented all the peaks of the not hydrated sodium aluminate crystalline phase (oP16, PCD n°313636). However, at 42.36 ° a peak referred to Na_2CO_3 (hP12 PCD n°1614691) was found, at 38.08, 41.20 and 44.57 reflections referred to Na_2CO_3 (mS24, PCD n°.1614701), were also found. In KI_A pattern no peaks of KI or K_2O have been detected, indicating that impregnation successfully introduced the precursors into the pores of the support. Detected peaks revealed that the support is constituted by γ-Al_2O_3 and, as often in commercial aluminas, also δ-Al_2O_3 phase seems to be present (tP160, PCD n°. 1800436). In CHT pattern, the principal phase seems to be constituted by $MgCO_3$, (hR30 PCD n°1040104), revealing that calcination step didn't efficiently removed carbonates. Also, a reflection that can be attributed to the presence of MgO cannot be excluded at ~ 43°, while characteristic features of mixed oxides structure (calcined hydrotalcites) were also detected. SrO seemed to be mainly constituted by SrO, (cF8 PCD n°1823306), $Sr(OH)_2$ (oP12, PCD n° 1415803)and $SrCO_3$, (oP20 PCD n°1920636). In particular, the presence of the hydroxide and carbonate confirmed the highly hygroscopic nature of the material that can easily adsorb moisture and environmental CO_2. Similarly, CaO diffraction pattern revealed the peaks of the pure oxide species cF8, (PCD n°1241063) with also the presence of $CaCO_3$ (hR30 PCD. n° 1140061).

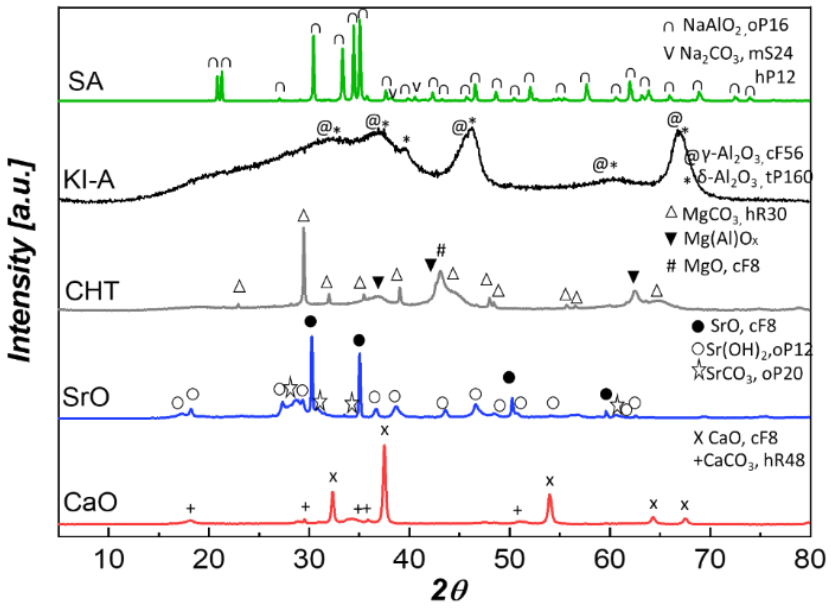

Figure 1: XRD patterns of the studied catalysts

The texture of the materials has been also investigated, in Figure 2, N_2 adsorption/desorption isotherms and pore size distribution curves are reported. BET surface area and pore volume values are included in Table 1. Considering Specific Surface Area (SSA), only KI_A showed a value equal to 171 m^2/g, typical of alumina-based materials. The other catalysts presented SSA < 20 m^2/g. Pore diameters reported in table 1 clearly revealed that mesoporosity is predominant although the pore volumes, except for KI_A, were always lower than 0.07 cm^3/g (insets C, D). Looking at inset A, KI_A and CHT isotherms well correspond with type IV isotherms, according to IUPAC classification[40], the loops showed, an intermediate shape in-between H1 and H2, probably due to a complex pore structure with network effects. The low surface A CaO exhibited a type IV isotherm, with a hysteresis loop that corresponds to type H1, that is usually associated with solids consisting of nearly cylindrical channels, agglomerates or uniform spherical particles[37]. Similarly, with even lower adsorbed quantity of N_2, SrO and SA hysteresis agreed with type IV isotherm. In fact, they showed narrow H1 loops, probably due to a limited range of uniform mesopores, with minimal network effects and a delayed condensation on the adsorption branch[40].

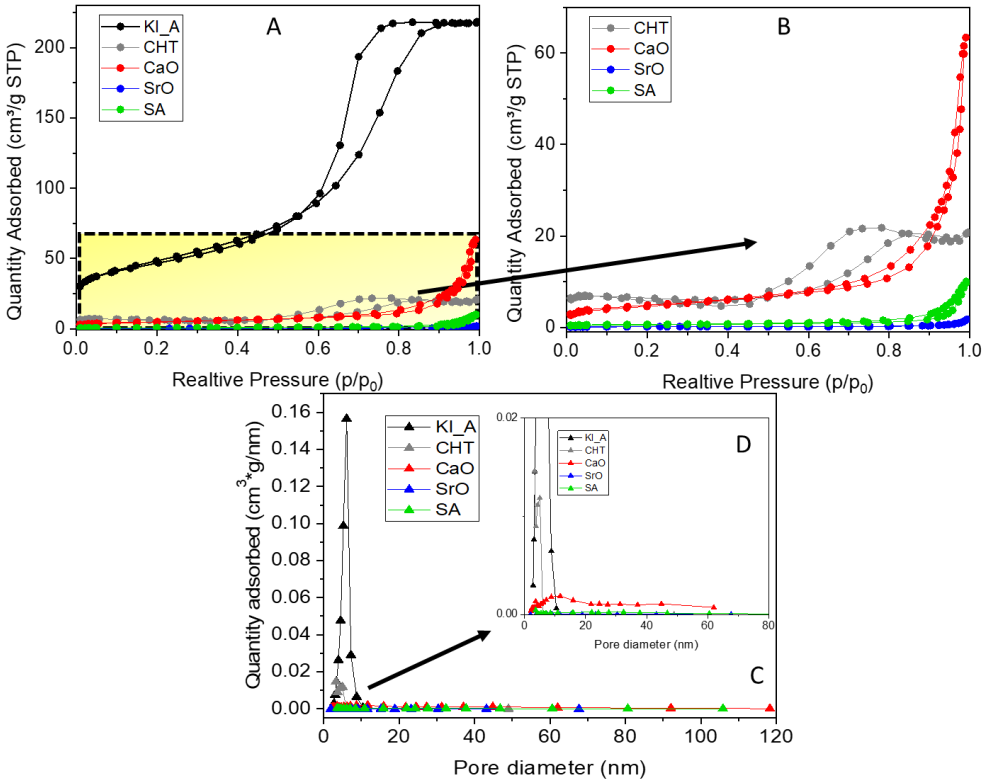

Figure 2: N_2 adsorption/desorption isotherms (insets A and B) and pore size distributions (C and D) of investigated catalysts

Table 1: Textural features and basicity values evaluated from TPD measurements

Catalyst	SSA (m^2/g)	P_d (nm)	P_v (cm^3*g)	Amount of CO_2 desorbed ($mmol/g_{cat}$)	Amount of CO_2 desorbed ($\mu mol/m^2$)
KI_A	171	6	0.34	0.02	1224
CHT	17	4	0.03	n.m.	122
CaO	16	20	0.07	0.18	115
SrO	0.5	26	0.02	0.11	4
SA	2	24	0.01	0.33	14

Note: SSA is the Specific Surface Area, P_d is the pore BJH desorption average pore diameter, P_v is the pore volume. n.m. not measured

Being that catalytic activity in the transesterification reaction is predominantly related to the basicity of the materials[41], the evaluation of the basic sites quantity and quality is pivotal. The amount of desorbed CO_2 and the temperature of maximum desorption are commonly recognized as important criteria for the amount and strength of basic sites. Thus, CO_2 temperature programmed desorption (TPD) measurements have been carried out and reported in Figure 3. It is well known that weak basic sites are generally related to CO_2 desorption temperatures < 673 K. KI_A and CHT show these characteristic features with broad band at 400 and 563 K. Considering the region of strong basic sites (T > 673 K) CaO, SrO and SA revealed more intense peaks at 876 K, 960 K and 1063 K, respectively. It appears clear that for SA the basicity is strongly superior, also considering the quantitative estimation of the sites reported in table 1 (0.33 vs 0.18 $mmol/g_{cat}$).

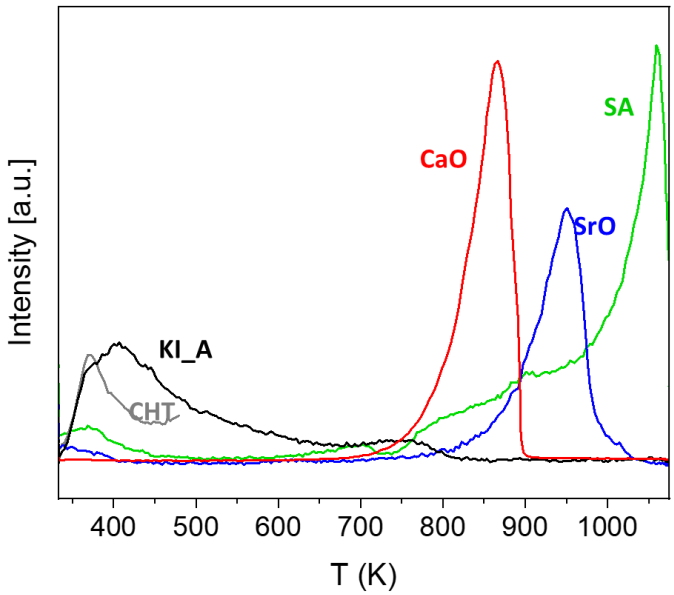

Figure 3: CO_2-TPD of the calcined catalysts

Carbon dioxide is commonly employed as probe molecule for basic catalysts because it easily reacts with surface oxygen or hydroxides species, giving rise to carbonate or bicarbonate species.

Nevertheless, the nature of strongly basic catalysts is often hygroscopic (easy moisture and CO_2 poison) and carbonates can be related to the surface or/and to the bulk. Thus, to further understand the nature of the basic sites and better demonstrate the structure of the catalysts a IR characterization has been carried out.

In Fig. 4 skeletal FT-IR spectra have been reported. νOH modes found at 3610-1650 cm^{-1}, 1630-1640 cm^{-1}, 1450 cm^{-1} were due to the presence of bicarbonate ions[42] $[HCO_3]^-$ and have been detected in CaO, SrO, SA, although surprisingly for the latter, the sharp band near 3600 wasn't detected. Trigonal geometry of CO_3^{2-} was also detected for two frequencies in the range 870-1050 cm^{-1} and a probable shoulder at 1420 in the band centered around 1450 cm^{-1} [43]. For CHT a sharp and intense absorption at 1387 cm^{-1} as well the shoulder at slightly higher frequencies can be attributed to the symmetrical carbonates. In full agreement with XRD patterns, these carbonates can be attributed at bulky species as well surface species. Broad absorptions in the range 3000-3600 cm^{-1} were due to O-H asymmetric stretches modes of water molecules adsorbed by the catalyst. It has to be noted that the strongest absorption centered at 3500 cm^{-1}in SrO, is probably due to the oxydryles vibrations of $Sr(OH)_2$ otherwise detected in XRD pattern.

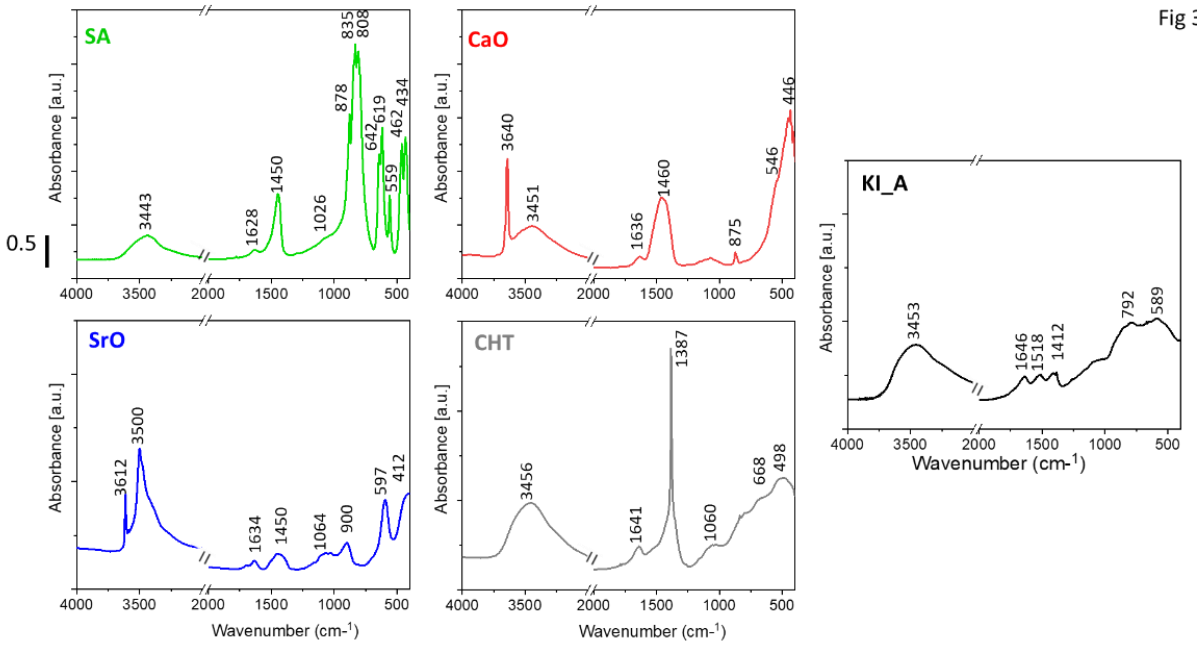

Figure 4: FT-IR skeletal spectra (KBr pressed disks) of the as prepared catalysts

In agreement with the identified crystalline structure, in Fig. 4, SA displayed stretching vibrations at 835 and 808 cm^{-1} and 642, 619 cm^{-1} due to AlO_4 tetrahedra, the absorption at 559 cm^{-1} is due to AlO_4-NaO_4 lattice vibrations, and the remaining bands at 462 and 434 cm^{-1} were attributed to complex mixed vibrations of the lattice[44]. Lattice vibrations, confirming the presence of the oxide, are also

found at 546 and 446 cm^{-1}, 597, 412 cm^{-1} for CaO and SrO respectively. Finally, broad absorptions in the range 500-900 cm^{-1} confirmed the γ-Al_2O_3 structure[45] for KI_A and the mixed oxide structure for CHT due to the presence of Mg–O and Al–O mixed bands[46].

To further explore basic sites typologies, present on the catalysts, CO_2 adsorption was studied by Diffuse Reflectance Infrared Fourier Transform Spectroscopy (DRIFTS, Figure 5). For sake of brevity adsorption and desorption spectra are reported in ESI. In Fig. 5 DRIFT spectra of the catalysts in test conditions (inset A) revealed the surface species that also act during the transesterification reaction while inset B permitted to detect effective weak species that are desorbed after hating at 673 K. In agreement with FT-IR spectra, catalysts in test conditions, i.e. the DRIFT spectrum, recorded immediately after the drying step, revealed the presence of different carbonates types, both weak and strong. The weak basic sites are normally referred to CO_2 molecules interacting with M^{2+}-O^{2-} and M^{3+}-O^{2-} pairs or to surface hydroxyl groups. To further explore the presence of these sites heating and recording spectra in an inert atmosphere is crucial. Thus, subtraction spectra (inset B) for CaO, SrO, CHT, KI_A revealed that in the region 1200-1800 cm^{-1} mainly weakly adsorbed carbonates, as bridged and bidentate or free ones[43,47], depending of the $\Delta\nu_3$ splitting, were removed. Moreover, hydroxyl species are also removed, except in the case of SrO and CaO, where probably bulk HCO_3^- species are found. Upon heating, SA loses hydroxyl species and weakly bonded bicarbonates (3000-3700 cm-1 band in inset B). Finally, in agreement with TPD measures, over SA, only weak absorptions were detected in the 1200-1800 cm^{-1} region, confirming the presence of almost strong basic sites (monodentates or polydentates), i.e. CO_2 molecules interacting with isolated O^{2-} anions, that are not desorbed after heating at 673 K.

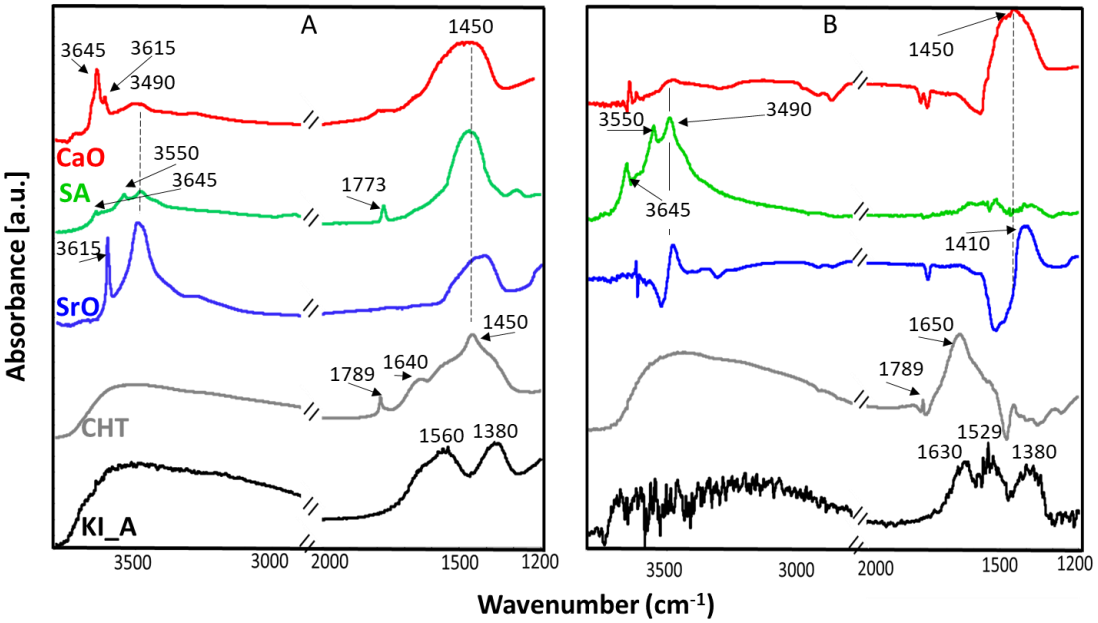

Figure 5: DRIFT spectra in test conditions (inset A) and DRIFT subraction spectra after heating at 673 K (inset B).

Catalytic activity

In figure 6 the FAME yield trend upon time is reported for all the catalysts. These results show that already after 20 minutes, SA had a yield of 37% to next increase upon almost equilibrium conditions. At the same time, CaO, CHT and KI_A obtain yields far lower than 20%. Additionally, at 60 min, SA, with a yield near 70%, almost doubled the other catalysts. Catalytic results are in full agreement with IR and TPD characterization, underlining a superior quantity and quality of basic sites for SA. On other hand, SrO, which seems to be really active, revealed a strange catalytic behavior because after 20 min essentially reached a plateau without going to full conversion. The behavior is confirmed by acid values titration (ESI Fig. 2) over reaction mix upon time: SrO is the only catalyst presenting an incremented acidity in terms of used mgNaOH to reach full neutralization. This is probably due to the dissolution of $Sr(OH)_2$, that while creating CH_3O^- species produces also H_2O molecules able to provoke the hydrolysis of the esters and thus generating Free Fatty Acids (FFA). Furthermore, the catalyst is almost totally dissolved in the reaction media after only 3 min of reaction. Finally, ICP-MS analyses confirmed noticeable Sr% already after 3 min in the reaction media (ESI Fig 3).

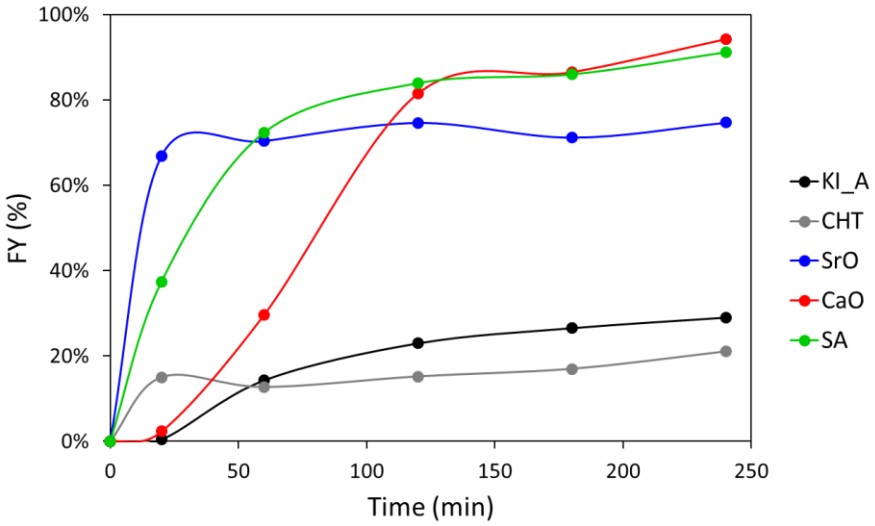

Figure 6: Catalytic activity of the studied catalysts.

Although CaO present excellent FAME yield values, it has to be noticed that the activity can be related to the fact that surfaces sites are not poisoned by environmental CO_2 or H_2O. In fact, it has been continuously stored in a vacuum oven to prevent poisoning and in agreements with considered precautions in the reference. To furtherly prove the effectiveness of SA, CaO was tested again after a storage period without vacuum, as well in the same conditions of SA. Obtained data (ESI Fig. 3)

confirmed that also a limited contact with the environment (the catalysts have been sealed and stored in desiccator) poisoned CaO catalyst and reduced the FAME yield. Finally, CaO competed with yield values similar to SA only after 120 min of reaction.

To better compare the catalysts in terms of intrinsic basicity it is meaningful to relate initial catalytic activities, i.e., after 20 min, respect to the quantity of strong basic sites, evaluated by TPD per grams of catalyst, and respect to the surface basicity evaluated by CO_2 adsorbed molecules per m^2 (Figure 7). It appears clear that catalysts can have a high surface basicity (i.e., KI_A) without being active because of the low density and/or strength of these sites. Being that the compared catalysts have textural properties that are different and being that equal grams were used in each test, basicity per grams seems to be fundamental respect to basicity per m^2. Except for SrO that is not suitable because of its solubility, SA showed the best catalytic activity as a compromise of a high basic density and a low surface basicity. In fact, it is the most active catalyst with an initial activity (20 min) that is at least more than two times active respect to the other catalysts.

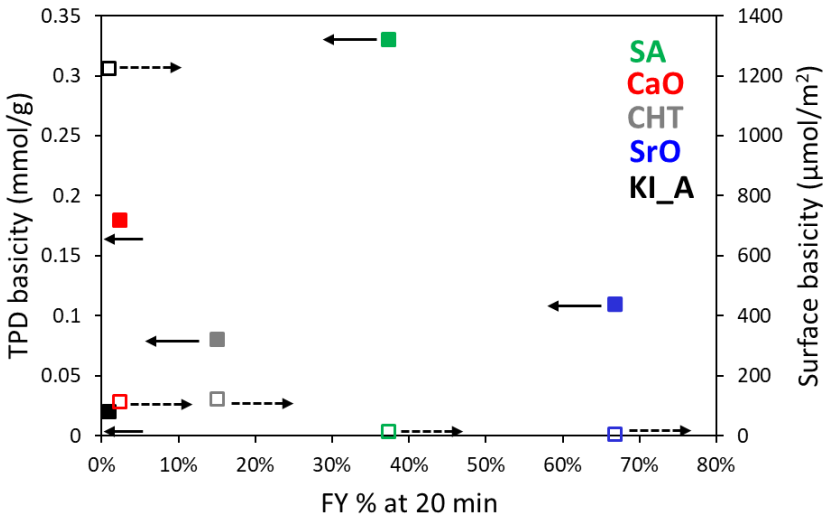

Figure 7: Correlation between the initial catalytic activity and surface basicity and TPD basicity.

For heterogeneous catalysis in liquid phase the leaching of solid is often a recurring problem and it has to be necessarily avoided. To proof the immiscibility of the investigated catalysts in the reaction media, hot filtration tests have been carried out and reported in Fig. 8. SA, CaO and CHT, after the catalyst removal, didn't show any incremented FAME yield, sign that reaction is essentially stopped without the catalyst. For KI_A, after its removal, it is clear that reaction is anyway proceeding. According also to literature[48,49], it is possible to affirm that the leaching of K-based species occurred, moreover confirmed by the fact that reaction mix changed in color from pale yellow to dark yellow.

Finally, SrO trend confirmed an almost homogeneous behavior, achieving yield values practically identical to the reaction from which no catalyst was removed.

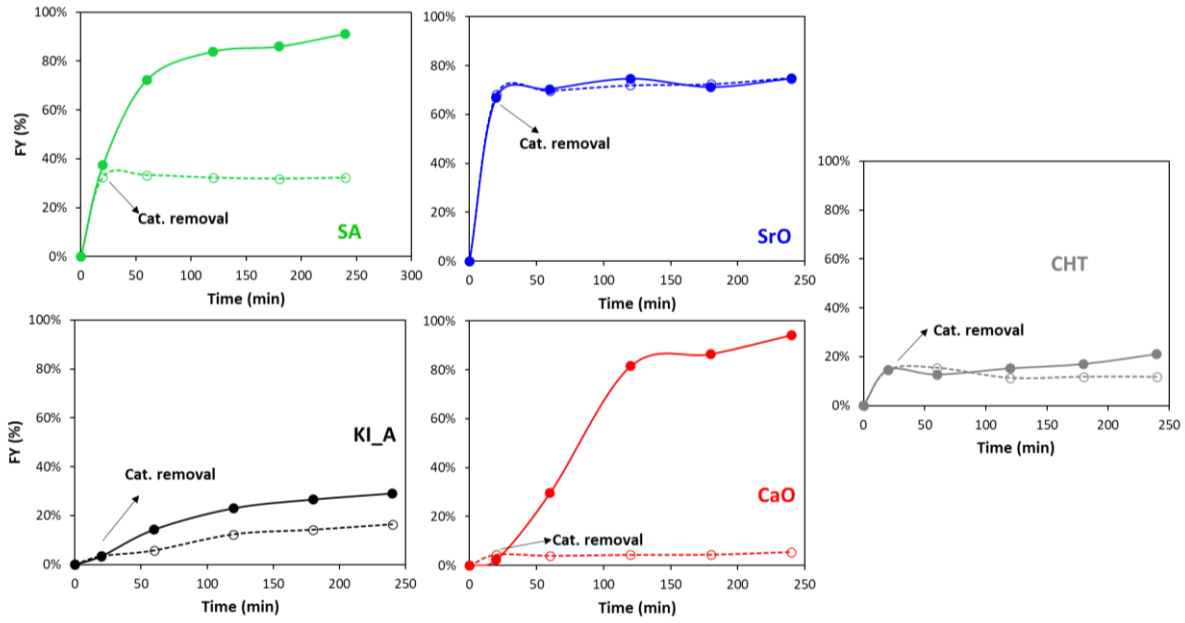

Figure 8: hot filtration tests for the studied catalysts.

Another key point for sustainability in the heterogeneous catalyzed process is the reusability of the catalyst, aiming to reduce costs and wastes. SA has been tested for 4 consequent times in the same experimental conditions (see ESI Fig. 4) and a slow decrement, in the catalytic activity is found at the end of the tests. Heat treatments to rejuvenate the catalyst can easily remove organic poisons although they probably lead to a progressive catalyst deactivation by sintering. Moreover, it has to be noticed that, a) even after 4 cycles, SA is still more active than the other catalysts at the first run and b) because of its cheapness and availability it could be easily replaced.

Finally, being that SA seems to be the most active and promising catalyst among the studied ones (and it does not suffer of leaching) another catalytic comparison has been foreseen. In fact, to assess a real possibility for the scale up step, it's mandatory to compare it with a homogeneous catalyst that is normally employed in industrial transesterification processes, i.e. NaOH. In Fig. 9 the catalytic comparison between SA and NaOH, in terms of same basic sites (evaluated by CO_2-TPD) is reported. Except for the first 20 min where, because of its homogeneous nature, NaOH obviously achieved the highest yield value, SA outcompeted with the progress of time.

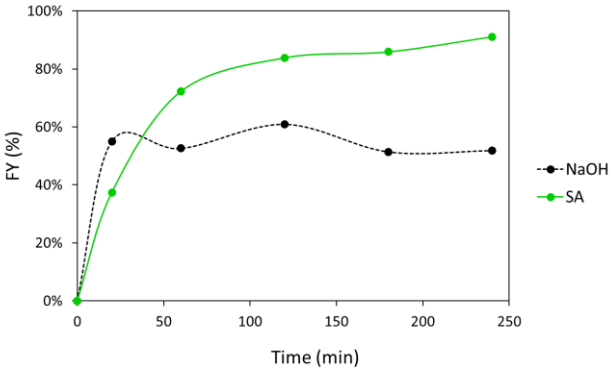

Figure 9: Catalytic comparison of SA with NaOH (homogeneous catalyst) considering the same amount of basic catalytic sites.

Equilibrium limitation around 55-60% for NaOH are probably due to the acidity of the oil, i.e. 1.12 mgNaOH* g of oil (see also ESI Fig. 2), that is slightly higher than the recommended limit of 1mgNaOH*g of oil[50]. In fact, one of the most important drawbacks for homogeneous catalysts is the feedstock purity[13]. A high content in FFA lead to easily produce soap and then reduce the amount of effectively available catalyst for the transesterification reaction[51]. Furthermore, NaOH is highly hygroscopic, and moisture can easily poison the catalyst. The consequence is a reduced yield and, at industrial level, high costs of separation and purification.

CONLCUSIONS

The main conclusions are:

- Different strongly basic catalysts have been characterized, tested and compared in the same experimental conditions for the Biodiesel synthesis.
- Among these Sodium Aluminate is the most catalytically active. It's strongly basic, the basicity is both due to a high quantity of basic sites and to a qualitatively strong basic site.
- It is cheap and largely available as byproduct or recoverable, considering a circular economy approach, from many industrial processes.
- It outcompetes with homogeneous catalysts, in the same conditions and with the same quantity of basic sites because produce no soap and it is not deactivated.

REFERENCES

(1) Hii, K. K.; Moores, A.; Pradeep, T.; Sels, B.; Allen, D. T.; Licence, P.; Subramaniam, B. Expectations for Manuscripts on Catalysis in ACS Sustainable Chemistry & Engineering. *ACS Sustainable Chemistry and Engineering*. American Chemical Society April 6, 2020, pp 4995–4996. https://doi.org/10.1021/acssuschemeng.0c01677.

(2) Estevez, R.; Aguado-Deblas, L.; Bautista, F. M.; Luna, D.; Luna, C.; Calero, J.; Posadillo, A.; Romero, A. A. Biodiesel at the Crossroads: A Critical Review. *Catalysts 2019, Vol. 9, Page 1033* **2019**, *9* (12), 1033. https://doi.org/10.3390/CATAL9121033.

(3) Moser, B. R. Biodiesel Production, Properties, and Feedstocks. *In Vitro Cellular & Developmental Biology - Plant 2009 45:3* **2009**, *45* (3), 229–266. https://doi.org/10.1007/S11627-009-9204-Z.

(4) Mandari, V.; Devarai, S. K. Biodiesel Production Using Homogeneous, Heterogeneous, and Enzyme Catalysts via Transesterification and Esterification Reactions: A Critical Review. *Bioenergy Research* **2022**, *15* (2), 935. https://doi.org/10.1007/S12155-021-10333-W.

(5) Chouhan, A. P. S.; Sarma, A. K. Modern Heterogeneous Catalysts for Biodiesel Production: A Comprehensive Review. *Renewable and Sustainable Energy Reviews* **2011**, *15* (9), 4378–4399. https://doi.org/10.1016/J.RSER.2011.07.112.

(6) Lam, M. K.; Lee, K. T.; Mohamed, A. R. Homogeneous, Heterogeneous and Enzymatic Catalysis for Transesterification of High Free Fatty Acid Oil (Waste Cooking Oil) to Biodiesel: A Review. *Biotechnology Advances* **2010**, *28* (4), 500–518. https://doi.org/10.1016/J.BIOTECHADV.2010.03.002.

(7) Xie, W.; Huang, X. Synthesis of Biodiesel from Soybean Oil Using Heterogeneous KF/ZnO Catalyst. *Catalysis Letters* **2006**, *107* (1–2), 53–59. https://doi.org/10.1007/S10562-005-9731-0.

(8) Ma, H.; Li, S.; Wang, B.; Wang, R.; Tian, S. Transesterification of Rapeseed Oil for Synthesizing Biodiesel by K/KOH/γ-Al_2O_3 as Heterogeneous Base Catalyst. *JAOCS, Journal of the American Oil Chemists' Society* **2008**, *85* (3), 263–270. https://doi.org/10.1007/S11746-007-1188-4.

(9) Salinas, D.; Araya, P.; Guerrero, S. Study of Potassium-Supported TiO2 Catalysts for the Production of Biodiesel. *Applied Catalysis B: Environmental* **2012**, *117–118*, 260–267. https://doi.org/10.1016/J.APCATB.2012.01.016.

(10) Du, L.; Li, Z.; Ding, S.; Chen, C.; Qu, S.; Yi, W.; Lu, J.; Ding, J. Synthesis and Characterization of Carbon-Based MgO Catalysts for Biodiesel Production from Castor Oil. *Fuel* **2019**, *258*, 116122. https://doi.org/10.1016/J.FUEL.2019.116122.

(11) López, D. E.; Goodwin, J. G.; Bruce, D. A.; Lotero, E. Transesterification of Triacetin with Methanol on Solid Acid and Base Catalysts. *Applied Catalysis A: General* **2005**, *295* (2), 97–105. https://doi.org/10.1016/J.APCATA.2005.07.055.

(12) Margellou, A.; Koutsouki, A.; Petrakis, D.; Vaimakis, T.; Manos, G.; Kontominas, M.; Pomonis, P. J. Enhanced Production of Biodiesel over MgO Catalysts Synthesized in the Presence of Poly-Vinyl-Alcohol (PVA). *Industrial Crops and Products* **2018**, *114*, 146–153. https://doi.org/10.1016/J.INDCROP.2018.01.079.

(13) Jamil, F.; Murphin Kumar, P. S.; Al-Haj, L.; Tay Zar Myint, M.; Al-Muhtaseb, A. H. Heterogeneous Carbon-Based Catalyst Modified by Alkaline Earth Metal Oxides for Biodiesel Production: Parametric and Kinetic Study. *Energy Conversion and Management: X* **2021**, *10*, 100047. https://doi.org/10.1016/J.ECMX.2020.100047.

(14) Das, V.; Tripathi, A. M.; Borah, M. J.; Dunford, N. T.; Deka, D. Cobalt-Doped CaO Catalyst Synthesized and Applied for Algal Biodiesel Production. *Renewable Energy* **2020**, *161*, 1110–1119. https://doi.org/10.1016/J.RENENE.2020.07.040.

(15) Li, H.; Wang, Y.; Ma, X.; Wu, Z.; Cui, P.; Lu, W.; Liu, F.; Chu, H.; Wang, Y. A Novel Magnetic CaO-Based Catalyst Synthesis and Characterization: Enhancing the Catalytic Activity and Stability of CaO for Biodiesel Production. *Chemical Engineering Journal* **2020**, *391*, 123549. https://doi.org/10.1016/J.CEJ.2019.123549.

(16) Tang, Y.; Xu, J.; Zhang, J.; Lu, Y. Biodiesel Production from Vegetable Oil by Using Modified CaO as Solid Basic Catalysts. *Journal of Cleaner Production* **2013**, *42*, 198–203. https://doi.org/10.1016/J.JCLEPRO.2012.11.001.

(17) Chantrasa, A.; Phlernjai, N.; Goodwin, J. G. Kinetics of Hydrotalcite Catalyzed Transesterification of Tricaprylin and Methanol for Biodiesel Synthesis. *Chemical Engineering Journal* **2011**, *168* (1), 333–340. https://doi.org/10.1016/J.CEJ.2011.01.033.

(18) Benedictto, G. P.; Sotelo, R. M.; Dalla Costa, B. O.; Fetter, G.; Basaldella, E. I. Potassium-Containing Hydroxylated Hydrotalcite as Efficient Catalyst for the Transesterification of Sunflower Oil. *Journal of Materials Science* **2018**, *53* (18), 12828–12836. https://doi.org/10.1007/S10853-018-2581-0/TABLES/3.

(19) Cantrell, D. G.; Gillie, L. J.; Lee, A. F.; Wilson, K. Structure-Reactivity Correlations in MgAl Hydrotalcite Catalysts for Biodiesel Synthesis. *Appl Catal A* **2005**, *287* (2), 183–190. https://doi.org/10.1016/j.apcata.2005.03.027.

(20) Reyero, I.; Velasco, I.; Sanz, O.; Montes, M.; Arzamendi, G.; Gandía, L. M. Structured Catalysts Based on Mg–Al Hydrotalcite for the Synthesis of Biodiesel. *Catal Today* **2013**, *216*, 211–219. https://doi.org/10.1016/j.cattod.2013.04.022.

(21) *Sodium Aluminate AluSAL Solution for Water Treatment - Alumichem*. https://alumichem.com/our-products/chemistry/aluminum-chemicals/sodium-aluminate-alusal/ (accessed 2022-06-28).

(22) Rayzman, V.; Filipovich, I.; Nisse, L.; Vlasenko, Y. Sodium Aluminate from Alumina-Bearing Intermediates and Wastes. *JOM 1998 50:11* **1998**, *50* (11), 32–37. https://doi.org/10.1007/S11837-998-0284-8.

(23) *US4668485A - Recovery of sodium aluminate from Bayer process red mud - Google Patents*. https://patents.google.com/patent/US4668485A/en (accessed 2022-06-28).

(24) Ramesh, S.; Devred, F.; Debecker, D. P. $NaAlO_2$ Supported on Titanium Dioxide as Solid Base Catalyst for the Carboxymethylation of Allyl Alcohol with DMC. *Applied Catalysis A: General* **2019**, *581*, 31–36. https://doi.org/10.1016/J.APCATA.2019.05.017.

(25) Ramesh, S.; Indukuri, K.; Riant, O.; Debecker, D. P. Synthesis of Carbonate Esters by Carboxymethylation Using $NaAlO_2$ as a Highly Active Heterogeneous Catalyst. *Organic Process Research and Development* **2018**, *22* (12), 1846–1851.

https://doi.org/10.1021/ACS.OPRD.8B00333/ASSET/IMAGES/MEDIUM/OP-2018-003337_0007.GIF.

(26) Ramesh, S.; Devred, F.; van den Biggelaar, L.; Debecker, D. P. Hydrotalcites Promoted by $NaAlO_2$ as Strongly Basic Catalysts with Record Activity in Glycerol Carbonate Synthesis. *ChemCatChem* **2018**, *10* (6), 1398–1405. https://doi.org/10.1002/CCTC.201701726.

(27) Rittiron, P.; Niamnuy, C.; Donphai, W.; Chareonpanich, M.; Seubsai, A. Production of Glycerol Carbonate from Glycerol over Templated-Sodium-Aluminate Catalysts Prepared Using a Spray-Drying Method. *ACS Omega* **2019**, *4* (5), 9001–9009. https://doi.org/10.1021/ACSOMEGA.9B00805.

(28) Chotchuang, A.; Kunsuk, P.; Phanpitakkul, A.; Chanklang, S.; Chareonpanich, M.; Seubsai, A. Production of Glycerol Carbonate from Glycerol over Modified Sodium-Aluminate-Doped Calcium Oxide Catalysts. *Catalysis Today* **2022**, *388–389*, 351–359. https://doi.org/10.1016/J.CATTOD.2020.06.007.

(29) Bai, R.; Liu, P.; Yang, J.; Liu, C.; Gu, Y. Facile Synthesis of 2-Aminothiophenes Using NaAlO2 as an Eco-Effective and Recyclable Catalyst. *ACS Sustainable Chemistry and Engineering* **2015**, *3* (7), 1292–1297. https://doi.org/10.1021/sc500763q.

(30) Yamanovskaya, I. A.; Kusova, T. v.; Kraev, A. S.; Agafonov, A. v.; Seisenbaeva, G. A.; Kessler, V. G. Formation of Mesoporous Structure in Al_2O_3–$NaAlO_2$-Based Materials Produced by Template Synthesis. *Journal of Sol-Gel Science and Technology* **2019**, *92* (2), 293–303. https://doi.org/10.1007/S10971-019-05039-7/FIGURES/8.

(31) Agafonov, A. v.; Yamanovskaya, I. A.; Ivanov, V. K.; Seisenbaeva, G. A.; Kessler, V. G. Controlling Micro- and Nanostructure and Activity of the $NaAlO_2$ Biodiesel Transesterification Catalyst by Its Dissolution in a Mesoporous γ-Al_2O_3-Matrix. *Journal of Sol-Gel Science and Technology* **2015**, *76* (1), 90–97. https://doi.org/10.1007/S10971-015-3755-8.

(32) Ning, Y.; Niu, S.; Wang, Y.; Zhao, J.; Lu, C. Sono-Modified Halloysite Nanotube with NaAlO2 as Novel Heterogeneous Catalyst for Biodiesel Production: Optimization via GA_BP Neural Network. *Renewable Energy* **2021**, *175*, 391–404. https://doi.org/10.1016/j.renene.2021.04.135.

(33) Tao, W.; Ping, Y.; Shenggang, W.; Yunbai, L. Application of Sodium Aluminate as a Heterogeneous Base Catalyst for Biodiesel Production from Soybean Oil. *Energy and Fuels* **2009**, *23* (2), 1089–1092. https://doi.org/10.1021/EF800904B.

(34) Mutreja, V.; Singh, S.; Ali, A. Sodium Aluminate as Catalyst for Transesterification of Waste Mutton Fat. *J Oleo Sci* **2012**, *61* (11), 665–669. https://doi.org/10.5650/JOS.61.665.

(35) Cherikkallinmel, S. K.; Gopalakrishnan, A.; Yaakob, Z.; Ramakrishnan, R. M.; Sugunan, S.; Narayanan, B. N. Sodium Aluminate from Waste Aluminium Source as Catalyst for the Transesterification of Jatropha Oil. *RSC Advances* **2015**, *5* (57), 46290–46294. https://doi.org/10.1039/C5RA05982H.

(36) Liu, X.; He, H.; Wang, Y.; Zhu, S. Transesterification of Soybean Oil to Biodiesel Using SrO as a Solid Base Catalyst. *Catalysis Communications* **2007**, *8* (7), 1107–1111. https://doi.org/10.1016/j.catcom.2006.10.026.

(37) Yoosuk, B.; Udomsap, P.; Puttasawat, B.; Krasae, P. Modification of Calcite by Hydration-Dehydration Method for Heterogeneous Biodiesel Production Process: The Effects of Water on Properties and Activity. *Chemical Engineering Journal* **2010**, *162* (1), 135–141. https://doi.org/10.1016/j.cej.2010.05.013.

(38) Xie, W.; Li, H. Alumina-Supported Potassium Iodide as a Heterogeneous Catalyst for Biodiesel Production from Soybean Oil. *Journal of Molecular Catalysis A: Chemical* **2006**, *255* (1–2), 1–9. https://doi.org/10.1016/j.molcata.2006.03.061.

(39) Zeng, H. yan; Feng, Z.; Deng, X.; Li, Y. qin. Activation of Mg-Al Hydrotalcite Catalysts for Transesterification of Rape Oil. *Fuel* **2008**, *87* (13–14), 3071–3076. https://doi.org/10.1016/j.fuel.2008.04.001.

(40) Thommes, M.; Kaneko, K.; Neimark, A. v; Olivier, J. P.; Rodriguez-Reinoso, F.; Rouquerol, J.; Sing, K. S. W. IUPAC Technical Report Physisorption of Gases, with Special Reference to the Evaluation of Surface Area and Pore Size Distribution (IUPAC Technical Report). *Pure Appl. Chem* **2015**, aop. https://doi.org/10.1515/pac-2014-1117.

(41) Lee, A. F.; Wilson, K. Recent Developments in Heterogeneous Catalysis for the Sustainable Production of Biodiesel. *Catalysis Today* **2015**, *242* (Part A), 3–18. https://doi.org/10.1016/J.CATTOD.2014.03.072.

(42) Busca, G. Bases and Basic Materials in Chemical and Environmental Processes. Liquid versus Solid Basicity. *Chemical Reviews* **2010**, *110* (4), 2217–2249. https://doi.org/10.1021/CR9000989/ASSET/CR9000989.FP.PNG_V03.

(43) Busca, G.; Lorenzelli, V. Infrared Spectroscopic Identification of Species Arising from Reactive Adsorption of Carbon Oxides on Metal Oxide Surfaces. *Materials Chemistry* **1982**, *7* (1), 89–126. https://doi.org/10.1016/0390-6035(82)90059-1.

(44) Tarte, P. Infra-Red Spectra of Inorganic Aluminates and Characteristic Vibrational Frequencies of AlO4 Tetrahedra and AlO6 Octahedra. *Spectrochimica Acta Part A: Molecular Spectroscopy* **1967**, *23* (7), 2127–2143. https://doi.org/10.1016/0584-8539(67)80100-4.

(45) Boumaza, A.; Favaro, L.; Lédion, J.; Sattonnay, G.; Brubach, J. B.; Berthet, P.; Huntz, A. M.; Roy, P.; Tétot, R. Transition Alumina Phases Induced by Heat Treatment of Boehmite: An X-Ray Diffraction and Infrared Spectroscopy Study. *Journal of Solid State Chemistry* **2009**, *182* (5), 1171–1176. https://doi.org/10.1016/J.JSSC.2009.02.006.

(46) López, T.; Bosch, P.; Asomoza, M.; Gómez, R.; Ramos, E. DTA-TGA and FTIR Spectroscopies of Sol-Gel Hydrotalcites: Aluminum Source Effect on Physicochemical Properties. *Materials Letters* **1997**, *31* (3–6), 311–316. https://doi.org/10.1016/S0167-577X(96)00296-0.

(47) Coenen, K.; Gallucci, F.; Mezari, B.; Hensen, E.; van Sint Annaland, M. An In-Situ IR Study on the Adsorption of CO2 and H2O on Hydrotalcites. *Journal of CO2 Utilization* **2018**, *24*, 228–239. https://doi.org/10.1016/J.JCOU.2018.01.008.

(48) Alonso, D. M.; Mariscal, R.; Moreno-Tost, R.; Poves, M. D. Z.; Granados, M. L. Potassium Leaching during Triglyceride Transesterification Using K/γ-Al2O3 Catalysts. *Catalysis Communications* **2007**, *8* (12), 2074–2080. https://doi.org/10.1016/J.CATCOM.2007.04.003.

(49) Čapek, L.; Hájek, M.; Kutálek, P.; Smoláková, L. Aspects of Potassium Leaching in the Heterogeneously Catalyzed Transesterification of Rapeseed Oil. *Fuel* **2014**, *115*, 443–451. https://doi.org/10.1016/J.FUEL.2013.07.081.

(50) Moser, B. R. Biodiesel Production, Properties, and Feedstocks. *In Vitro Cellular and Developmental Biology - Plant* **2009**, *45* (3), 229–266. https://doi.org/10.1007/S11627-009-9204-Z.

(51) Changmai, B.; Vanlalveni, C.; Ingle, A. P.; Bhagat, R.; Rokhum, L. Widely Used Catalysts in Biodiesel Production: A Review. *RSC Advances* **2020**, *10* (68), 41625–41679. https://doi.org/10.1039/D0RA07931F.